Curr Microbiol (2008) 56:363–370
DOI 10.1007/s00284-007-9091-7

Production of Calcium Oxalate Crystals by the Basidiomycete *Moniliophthora perniciosa*, the Causal Agent of Witches' Broom Disease of Cacao

Maria Carolina S. do Rio · Bruno V. de Oliveira · Daniela P. T. de Tomazella · José A. Fracassi da Silva · Gonçalo A. G. Pereira

Received: 21 August 2007 / Accepted: 26 November 2007 / Published online: 3 January 2008

Abstract Oxalic acid has been shown as a virulence factor for some phytopathogenic fungi, removing calcium from pectin and favoring plant cell wall degradation. Recently, it was published that calcium oxalate accumulates in infected cacao tissues during the progression of Witches' Broom disease (WBD). In the present work we report that the hemibiotrophic basidiomycete *Moniliophthora perniciosa*, the causal agent of WBD, produces calcium oxalate crystals. These crystals were initially observed by polarized light microscopy of hyphae growing on a glass slide, apparently being secreted from the cells. The analysis was refined by Scanning electron microscopy and the compositon of the crystals was confirmed by energy-dispersive x-ray spectrometry. The production of oxalate by *M. perniciosa* was reinforced by the identification of a putative gene coding for oxaloacetate acetylhydrolase, which catalyzes the hydrolysis of oxaloacetate to oxalate and acetate. This gene was shown to be expressed in the biotrophic-like mycelia, which *in planta* occupy the intercellular middle-lamella space, a region filled with pectin. Taken together, our results suggest that oxalate production by *M. perniciosa* may play a role in the WBD pathogenesis mechanism.

M. C. S. do Rio · B. V. de Oliveira · D. P. T. de Tomazella · G. A. G. Pereira (✉)
Laboratório de Genômica e Expressão, Departamento de Genética e Evolução, Instituto de Biologia, Universidade Estadual de Campinas, CP 6109, Campinas 13083-970 São Paulo, Brazil
e-mail: goncalo@unicamp.br

J. A. F. da Silva
Departamento de Química Analítica, Instituto de Química, Universidade Estadual de Campinas, CP 6157, Campinas 13083-970 São Paulo, Brazil

Introduction

Moniliophthora perniciosa (Stahel) Aime & Phillips-Mora (*Agaricales, Marasmiaceae*; formerly *Crinipellis perniciosa* [Stahel] Singer) is the causal agent of witches' broom disease (WBD), one of the most important phytosanitary problems of cacao (*Theobroma cacao* L.) in the Americas [25, 29]. This fungus is believed to have originated in the Amazon basin and it is known to infect five families of dicotyledons, including Malvaceae and Solanaceae [8, 14, 25].

The biology of the *M. perniciosa*-cacao interaction is complex and has only recently been studied at the molecular level: a genome project for the fungus produced a draft sequence with twofold coverage (http://www.lge.ibi.unicamp.br/vassoura; work in progress). *M. perniciosa* exhibits a hemibiotrophic life cycle that parallels the symptoms in the plant. A monokaryotic biotrophic mycelium, without clamp connections, is formed after basiodiospore germination and infects flower cushions, developing fruit, and vegetative flushes. In the latter case, the infection causes hypertrophy, hyperplasia, and loss of apical dominance, producing a characteristic green broom structure [8, 9]. Remarkably, despite these symptoms, the biotrophic hyphae are found at low density [24] and do not produce haustoria, only occupying the apoplastic space and showing slow growth [3]. We have recently demonstrated that a biotrophic-like mycelia can be kept in vitro by growing spores under nutrient starvation and providing glycerol as a unique carbon source [27]. Therefore, the low nutrient concentration present in apoplast may be the key for the biotrophic phase. Moreover, during this phase, the infected tissue seems to be under intense oxidative stress, which is indicated by the increase in lipid peroxidation [27]. One possible reason for the existence of this oxidative

situation is the production of hydrogen peroxide by the enzymatic degradation of calcium oxalate crystals (COCs) present in infected plants, which seems to increase during the progression of the disease [3].

During the second (saprotrophic) phase of the life cycle, infected plant tissues become necrotic, forming dry brooms, and the fungus acquires some distinctive features such as the presence of a dikaryotic saprotrophic/necrotrophic mycelium, showing clamp connections [5, 29]. In contrast to the biotrophic hyphae, the saprotrophic mycelium grows vigorously, quickly colonizing the infected plant tissue. Elucidating the mechanisms responsible for the change from the biotrophic to the saprotrophic/necrotrophic phase of the fungus and understanding whether the death of the infected cacao tissue is a consequence or precedes this change in mycelial morphology and physiology is a central question that remains to be answered.

Calcium oxalate is a common constituent of plant cells and its oxidation is involved in plant defense [10]. Interestingly, some pathogens, like *Sclerotinia sclerotiorum*, secrete oxalic acid, which seems to have a role in removing calcium ions bound to host cell wall pectins, thus exposing these structures to enzymes produced by the fungus [7]. In addition, it favors plant cell degradation by shifting the pH of infected plant tissues close to the optimum for cell wall-degrading enzymes such as polygalacturonases, as demonstrated with the basidiomycete *Athelia rolfsii* (formerly *Sclerotium rolfsii*) [2]. Finally, oxalic acid inhibits stomatal closure at night, first, by stimulating accumulation of potassium and starch hydrolysis in guard cells and, second, by disrupting the ABA-dependent process in plants infected with *Sclerotinia sclerotiorum* [4]. Since the basidiospores of *M. perniciosa* are sensitive to UV radiation and invade plants through stomata at night [25], the production of oxalic acid by their hyphae could help in the infection process.

In this work, we show that in vitro mycelia of *M. perniciosa* produces COCs, indicating that this compound may play a role in WBD.

Materials and Methods

Fungal Strain and Growth Conditions

The strain used in this work was FA553, a pure culture derived from spores of the isolate CP02 [11, 26]. Twenty samples of necrotrophic mycelium of this strain were separately inoculated in 300 µl of MYEA medium [21]. The medium was dropped onto one end of common glass slides, which were maintained under sterile conditions on a 2% agar-water layer inside a petri dish, sealed with Parafilm (Pechiney Plastic Packaging). The hyphae initially grew on the malt medium drop and subsequently they colonized the whole glass slide (Fig. 1). The dishes were cultivated inside a BOD (Biochemical Oxygen Demand) incubator chamber at 25°C and they were observed 30 days after inoculation. Glass slides containing only the drop of MYEA medium were maintained under the same conditions as negative controls.

Light Microscopy

After the incubation period, the petri dishes were opened and the glass slides were removed and immediately observed under normal and polarized white light with an Olympus BX51 optical microscope. The relevant aspects were photographed with Kodak ProImage 100 film and the scales were obtained with the projection of a micrometric slide under the same conditions utilized in the illustrations.

Electron Microscopy and Microanalysis

Microanalyses were performed with a JEOL JSM-6360 scanning electron microscope, with energy-dispersive x-ray spectrometry (EDS), operated at an accelerated voltage of 20 kV. Pieces (2 × 2 cm^2) of the slides containing the

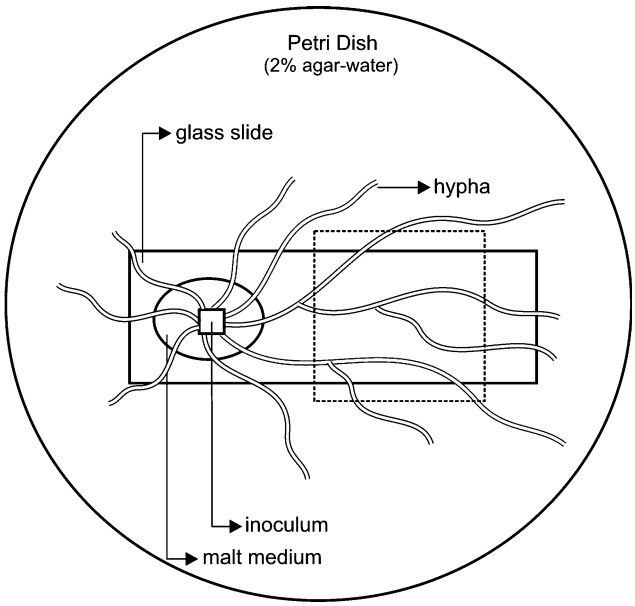

Fig. 1 Diagram showing the method used for growing necrotrophic mycelium of *M. perniciosa* on a common glass slide. The slide, with a drop of malt medium that had been inoculated with a small sample of *M. perniciosa* necrotrophic culture, was placed in a petri dish with a 2% agar-water layer, thus allowing the growth of the hyphae toward the edge of the dish [21]. After 1 month, the petri dishes were opened and the slides removed for microscopic evaluation, performed on the area indicated by the dashed square

hyphae but lacking the culture medium were cut with a diamond cutter and fixed on a carbon support with carbon tapes. In order to improve the image contrast, carbon was evaporated to form a thin (few nanometers) layer over the sample.

Results and Discussion

The hyphae growing on the glass slide, outside of the culture media, were analyzed by light microscopy. The original idea of this technique was to produce cells free of medium residues to stain nuclear DNA [21]. Remarkably, inspection of the necrotrophic mycelium led to the identification of well-defined tetragonal crystals near the hyphae (Fig. 2a), which were more evident when observed under polarized light (Fig. 2b). Identical structures had been detected associated with biotrophic-like mycelia growing on culture plates, indicating that they are also produced by this kind of hyphae. Glass slides incubated in the same way, but without fungi inoculation, did not produce any similar structure, indicating that this depended on cell activity. Reinforcing this view, we observed bright crystalline-like structures apparently being secreted by cells (Figs. 2c and d).

This analysis was refined by scanning electron microscopy (SEM). Several calcium-rich structures can be observed associated with the mycelium (Fig. 3a) in an image obtained with backscattered electrons (BECs). With BECs, image contrast dependent on the heavier elements is obtained. On closer inspection we observed that the crystals seem to be produced inside the hyphae (Figs. 3b-d), the

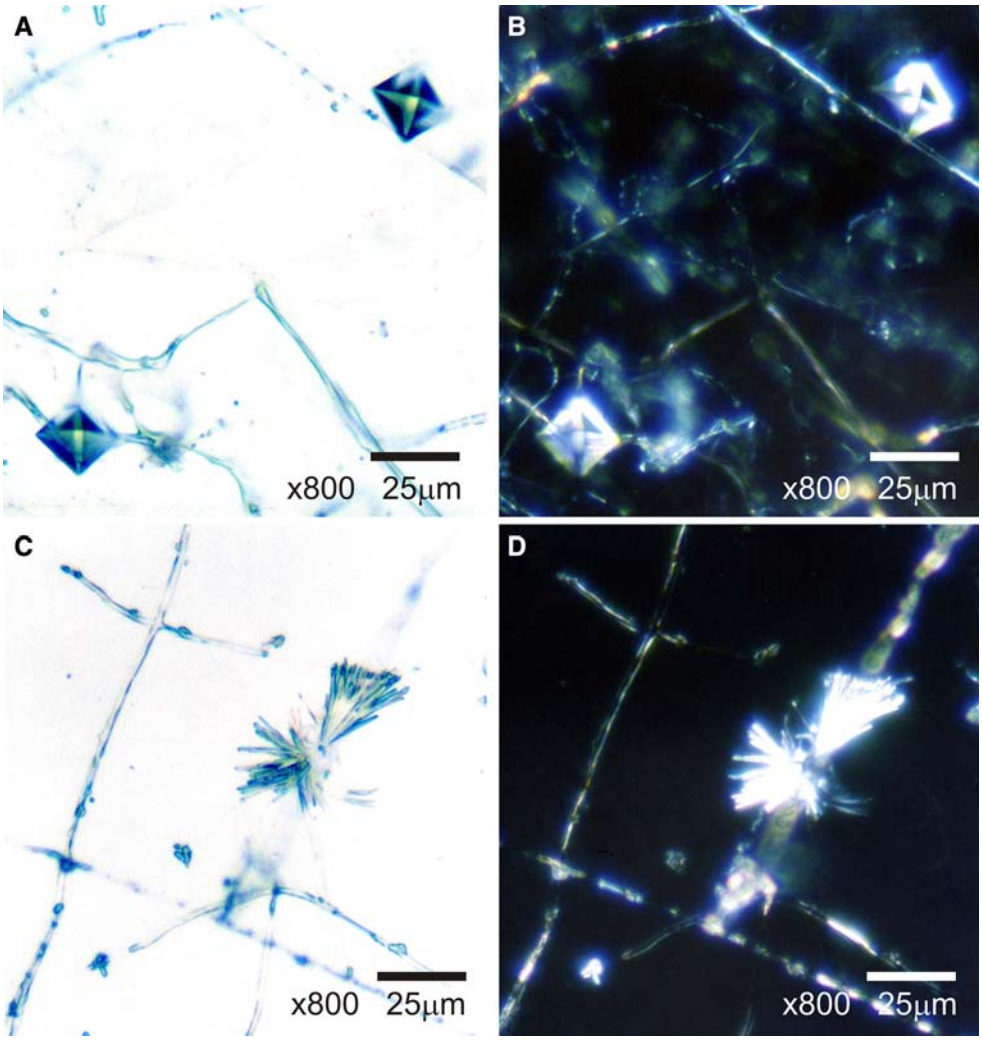

Fig. 2 Light microscopy of necrotrophic mycelium of *Moniliophthora perniciosa* without any treatment, showing crystalline structures associated with the hyphae. (**A, B**) Crystals of pyramidal shape of several sizes (2–20 µm) were observed. (**C, D**) Bright crystalline structures were registered apparently being secreted by the cells. The crystalline structures are more evident observed under polarized light (**B, D**)

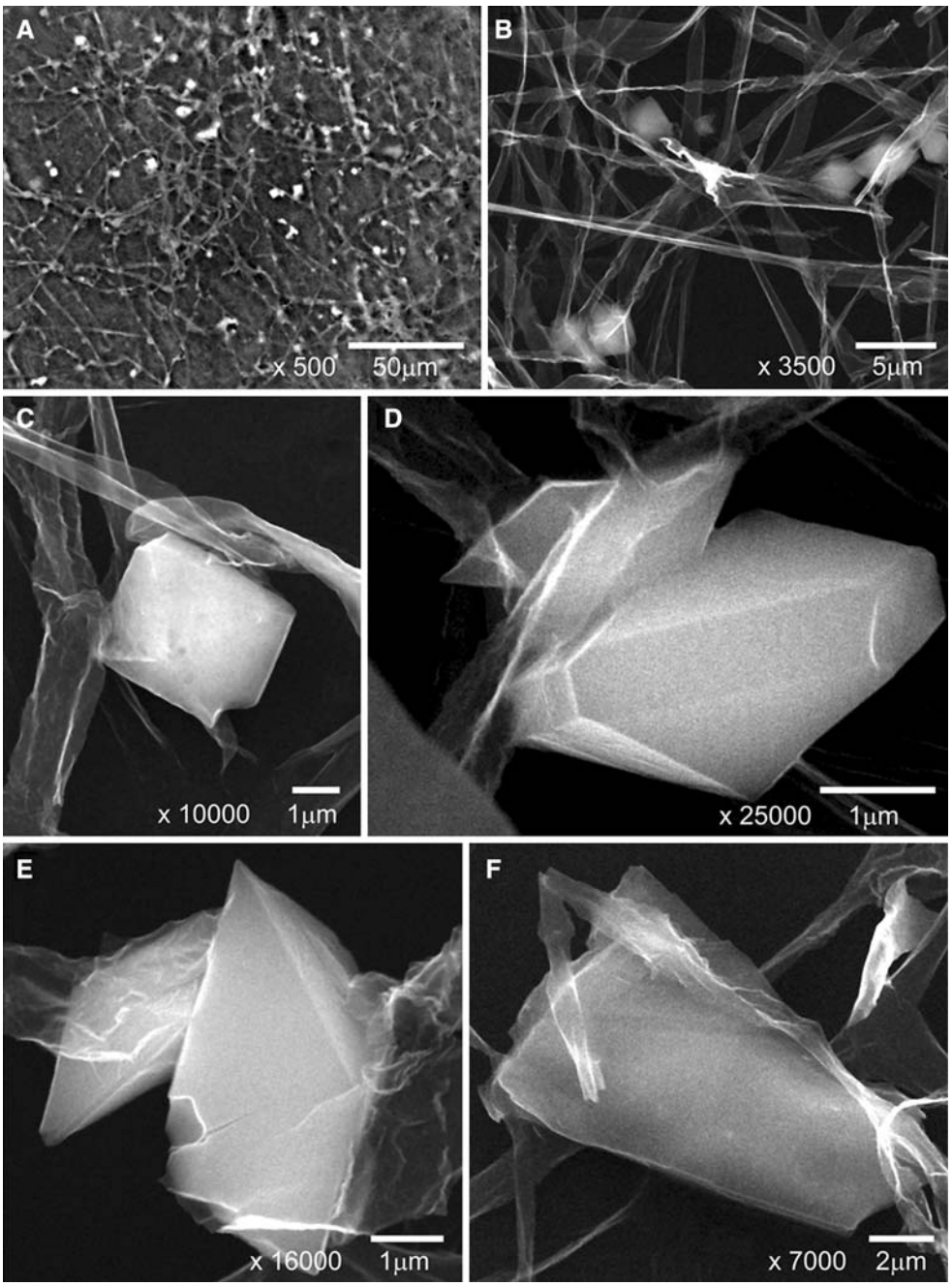

Fig. 3 SEM of *Moniliophthora perniciosa* necrotrophic mycelium. (**A**) Several calcium-rich structures can be observed associated with the mycelium, in an image obtained with backscattered electrons. (**B**) In a closer view, we observe that the crystals are produced inside the hyphae. (**C**) The pyramidal shape of the crystal, in a surface view. (**D**) Some crystals present a bipyramidal shape, due to the tetragonal system of growth (weddelite; dihydrated $CaC_2O_4.2H_2O$). (**E**) The crystals may cause rupture of the fungus cells. (**F**) Calcium oxalate crystals also grow in a monocyclic system (wewellite; monohydrate $CaC_2O_4.H_2O$)

growing of which may cause the cells to rupture (Fig. 3e and f).

Qualitative analysis using EDS is a powerful tool in microanalysis. Chemical analysis in SEM is performed by measuring the energy and intensity distribution of the x-ray signal generated by a focused electron beam [13]. Ideally, quantitative microanalysis would be the best choice to determine the crystal composition, but in this case it was not possible to perform an accurate and precise determination due to calibration difficulties. In any case, some qualitative conclusions can be obtained from the EDS data.

Qualitative analyses were performed in a comparative fashion, by positioning the electron beam over the crystal sample (signal sample; S_a) and over a region sufficiently

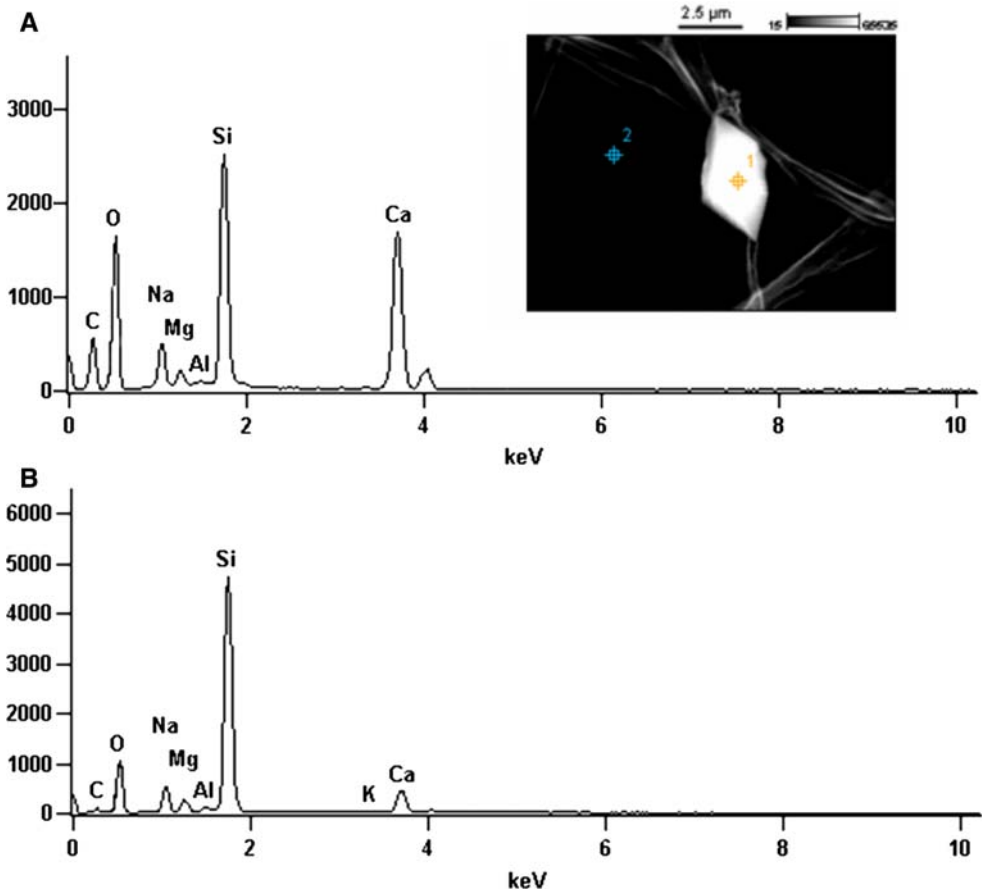

Fig. 4 Energy dispersive x-ray spectrometry (EDS) of the crystal sample. (**A**) EDS spectra obtained with the beam focused at point 1 (S_a) in the crystal sample (in detail at the top). (**B**) Beam focused at point 2 (S_b) for background signals. The inset shows the SEM image of the crystal sample, showing the location where the beam was focused

distant (signal blank; S_b). High-intensity peaks for oxygen, at ~0.5 keV, can be observed for both position S_a and position S_b (Fig. 4). The observed peak at S_b is due to the high oxygen content of the substrate. The greater intensity at S_a indicates that oxygen can be found in the crystal structure. It is worth noting the peaks for calcium (3.8 and 4.0 keV) and carbon (~0.2 keV). The high intensity of these peaks at S_a is strong evidence that calcium takes part in the composition of the crystal. Additionally, the presence of carbon suggests an anion containing this element: one can note the intensity of the carbon peak compared to the background. The presence of calcium in the background signal is due to the substrate composition. On the other hand, the small signal for carbon at S_b is due to the vapor deposition of this element during the sample preparation. The absence of peaks at higher energies (>5 keV) indicates that the lower-energy region, ranging up to 1 keV, does not suffer from interferences of heavier elements.

Some peaks appear with intensities closer to the operational limit of the instrument (background noise) and should not be considered for the purpose of qualitative analysis (Fig. 4). In this way, peaks attributed to Al, K, Na, and S were discarded. Again, the presence of traces of Al is probably due to the emission of X-rays from the atoms present in the construction of the microscope chamber. Beyond this, the electron beam has penetration greater than the sample dimensions, leading to the measurement of elements present on the supporting substrate. In this work the support was made by common glass slides, which are composed of silica (SiO_2) and silicates of alkaline and alkaline earth metals (essentially Na, Mg, and Ca). For silicon, x-rays generated at both position S_a and position S_b showed intensities of 21546 and 41137, respectively, which confirms that the silicon signal is due to the glass substrate. The beam penetration into the supporting substrate is less at position S_a, because the beam must pass through the crystal, which lowers the intensity at this point.

The possibility exists that the samples were formed by calcium carbonate, which has the same composition. However, this compound crystallizes as very small spheres, which were not observed in our analysis. In contrast, COCs are known to present pyramidal shapes, as a consequence of growing in the tetragonal system (weddellite; dihydrated $CaC_2O_4.2H_2O$). This structure was observed in our samples (Figs. 2 and 3).

The formation of COCs by basidiomycetes is not unusual and had been registered in the nonpathogenic fungi *Agaricus bisporus* and *Geastrum saccatum* [31, 32]. Moreover, many phytopathogenic filamentous fungi, such

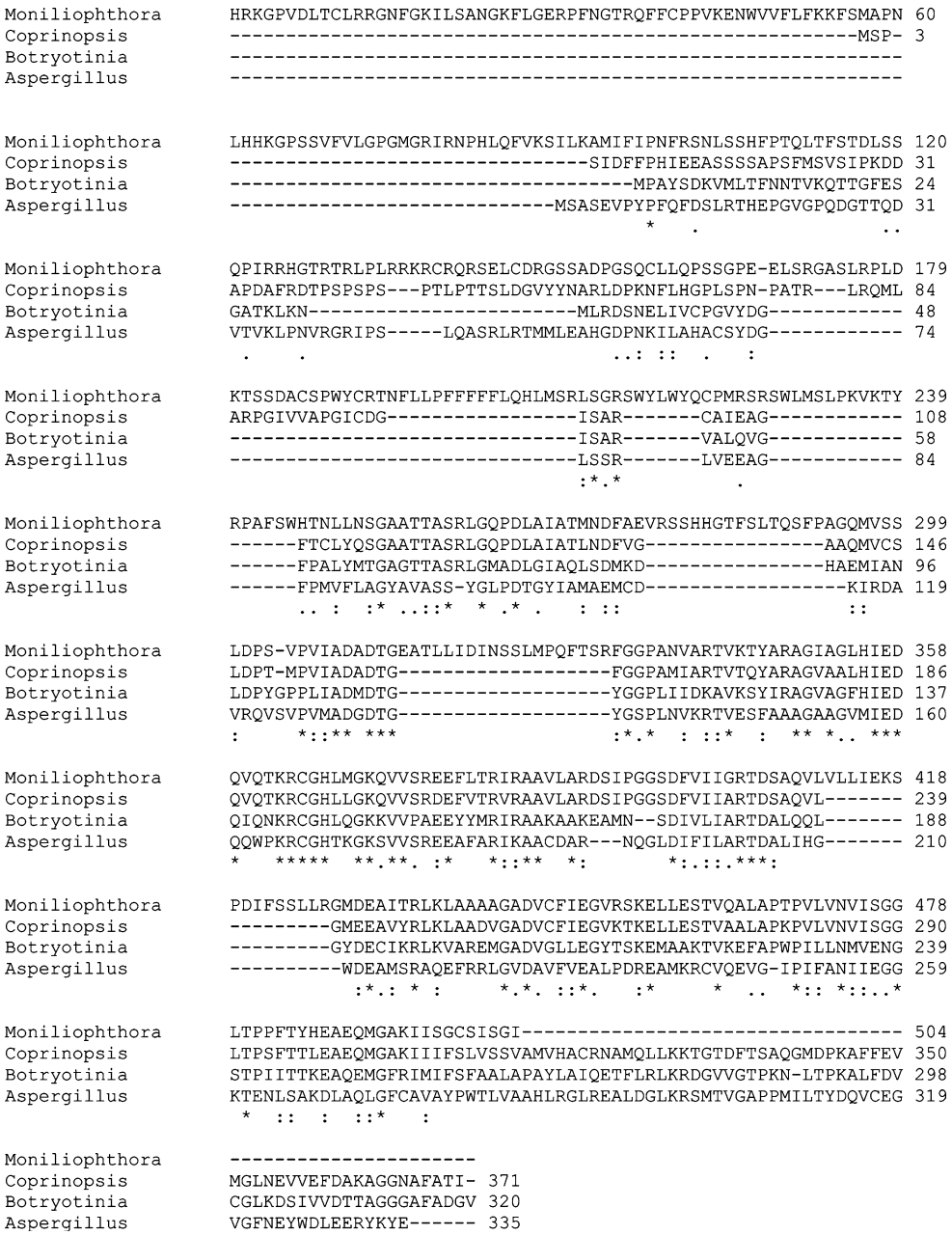

Fig. 5 Alignment of the amino acid sequence of predicted *Moniliophthora perniciosa* oxaloacetate acetylhydrolase (OAH; Gene Bank accession number EU179870) with the homologous *Coprinopsis cinerea* (Gene Bank accession number EAU91265; e-value, 0), *Botryotinia fuckeliana* (Gene Bank accession number AAS99938; e-value, $2e^{-43}$), and *Aspergillus niger* (Gene Bank accession number ABD78720; e-value, $2e^{-40}$). Activity of the enzyme was experimentally confirmed for the species *A. niger* and *B. fuckeliana*

as *Athelia rolfsii*, *Sclerotinia sclerotiorum*, and *Botrytis cinerea*, produce oxalate during interactions with their hosts [2, 4, 15, 16]. In fungi, oxalate can be synthesized from two possible substrates: oxaloacetate and glyoxylate. Oxaloacetate generated in the tricarboxylic acid cycle and in the glyoxylate cycle is hydrolyzed to oxalate and acetate in a reaction catalyzed by the enzyme oxaloacetate acetylhydrolase (OAH) [19]. Glyoxylate can be oxidized by the enzyme glyoxylate oxidase (GLOX) or dehydrogenized by the enzyme glyoxylate dehydrogenase (GLDH), generating oxalate in both cases [1, 30]. However, it has been reported that the oxaloacetate route is the main one for oxalate synthesis in most fungi [16, 18]. The wood-rotting basidiomycete *Fomitopsis palustris* shows both GLDH and OAH activities; however, OAH activity is five times higher than GLDH activity, demonstrating that oxalate is mainly produced from oxaloacetate [22].

Most oxalate-producing fungi exhibit only the OAH pathway. *S. sclerotiorum* expressed sequence tag (EST) libraries showed the presence of *oxaloacetate acetylhydrolase* (*oah*) expressed sequences during their interaction with *Bracassia napus* (canola); in contrast, *gldh* and *glox* sequences were not detected [28]. Moreover, deletion of the *oah*-encoding gene in *Aspergillus nidulans* and *Botrytis cinerea* resulted in total loss of oxalate production in both cases [16, 23].

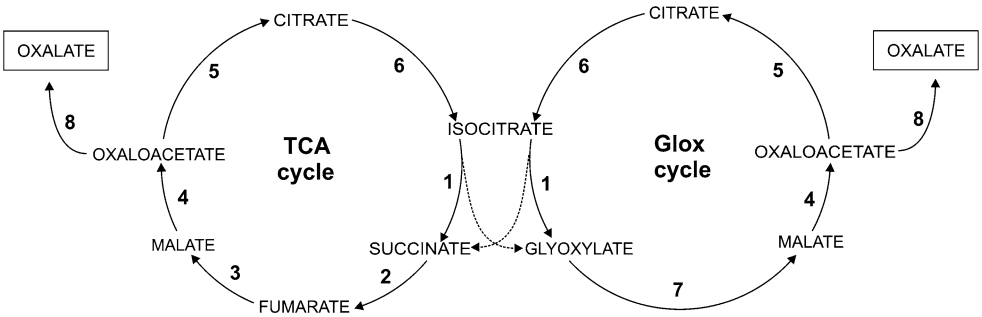

Fig. 6 Possible pathways for oxalate production in *Moniliophthora perniciosa*: (**1**) Isocitrate lyase; (**2**) succinate dehydrogenase; (**3**) fumarase; (**4**) malate dehydrogenase; (**5**) citrate sintase; (**6**) aconitate hydratase; (7) malate synthase; (8) oxaloacetate acetylhydrolase (OAH). TCA, tricarboxylic acid cycle; Glox, glyoxylate cycle

Therefore, since we have found that *M. perniciosa* produces calcium oxalate crystals, we should be able to find genes of this route in its genome. Indeed, we have found a sequence with high similarity to the *Coprinopsis cinerea*, *Botryotinia fuckeliana*, and *Aspergillus niger oah* genes (E-values: 0, $2e^{-43}$, and $2e^{-40}$, respectively) (Fig. 5). Most important, the EST corresponding to this gene was found in a library produced with RNA from in vitro biotrophic-like mycelia; therefore we conclude that *M. perniciosa* presents the gene responsible for the conversion of oxaloacetate to oxalate, and that, probably, this gene is also expressed in the biotrophic phase of the fungus *in planta*. Moreover, inspection of the genome led to the identification of all the enzymes necessary to produce oxaloacetate (Fig. 6). In summary, our data suggest that production of oxalate is a strategy employed in the establishment of WBD.

In fact, the presence of COCs in cacao tissues is observed during the development of WBD. There is an increase in the number of these crystals in infected seedlings, followed by a rapid decrease in the final stages of the disease [3]. High oxalate concentrations are toxic to cells because COC degradation by oxalate oxidase leads to H_2O_2 production. This compound has been found in infected tissues [3] and the germin oxalate oxidase gene has been proved to be expressed under these conditions [12].

Thus, the production of oxalate by *M. perniciosa* leading to the formation of calcium oxalate crystals could contribute to the increase in calcium oxalate contents in cacao tissues, as previously described. In addition, it may play an important role in all fungal stages, from the initial establishment of the fungus in the apoplast (biotrophic phase) to the final stages of WBD, characterized by the necrosis of the broom tissues (saprotrophic phase).

Diseases caused by fungi that produce oxalate have been successfully prevented with the use of transgenic plants expressing oxalate decarboxylase [6, 17]. For cacao, transgenic plants expressing chitinase have recently been obtained [20]. We believe that genes expressing enzymes that degrade oxalate should be tested in order to verify the effect of oxalate production in the progression of WBD.

Acknowledgments This work was supported by CNPq (Conselho Nacional de Desenvolvimento Científico e Tecnológico; No. 472279/2006-8) and FAPESP (Fundação de Amparo à Pesquisa do Estado de São Paulo; Nos. 06/50794-0, 06/59843-3, and 07/51030-6). The authors would like to thank Daniel Bratfisch Razzo for operation of the scanning electron microscope (JSM 6360 LV), Rafaela F. Camargo for help in preparing fungal samples, Dr. Francisco Javier Medrano for critical suggestions, and Dr. Johana Rincones and Dr. Carol H. Collins for manuscript revision.

References

1. Akamatsu Y, Ohta A, Takahashi M, et al. (1991) Enzymatic formation of oxalate from oxaloacetate with cell-free-extracts of the brown-rot fungus *Tyromyces palustris* in relation to the biodegradation of cellulose. Mokuzai Gakkaishi 37:575–577
2. Bateman DF, Beer SV (1965) Simultaneous production and synergistic action of oxalic acid and polygalacturonase during pathogenesis by *Sclerotium rolfsii*. Phytopathology 55:204
3. Ceita GO, Macêdo JNA, Santos TB, et al. (2007) Involvement of calcium oxalate degradation during programmed cell death in *Theobroma cacao* tissues triggered by the hemibiotrophic fungus *Moniliophthora perniciosa*. Plant Sci 173:106–117
4. Cessna SG, Sears VE, Dickman MB, et al. (2000) Oxalic acid, a pathogenicity factor for *Sclerotinia sclerotiorum*, suppresses the oxidative burst of the host plant. Plant Cell 12:2191–2199
5. Delgado JC, Cook AA (1976) Nuclear condition of basidia, basidiospores, and mycelium of *Marasmius perniciosus*. Can J Bot 54:66–72
6. Dias BBA, Cunha WG, Morais LS, et al. (2006) Expression of an oxalate decarboxylase gene from *Flammulina* sp. in transgenic lettuce (*Lactuca sativa*) plants and resistance to *Sclerotinia sclerotiorum*. Plant Pathol 55:187–193
7. Dutton MV, Evans CS (1996) Oxalate production by fungi: its role in pathogenicity and ecology in the soil environment. Can J Microbiol 42:881–895
8. Evans HC (1980) Pleomorphism in *Crinipellis perniciosa*, causal agent of witches broom disease of cocoa. Trans Br Mycol Soc 74:515–523
9. Evans HC, Bastos CN (1980) Basidiospore germination as a means of assessing resistance to *Crinipellis perniciosa* (Witches Broom Disease) in cocoa cultivars. Trans Bri Mycol Soc 74:525–536
10. Franceschi V (2001) Calcium oxalate in plants. Trends Plant Sci 6:331–331
11. Garcia O, Macedo JA, Tiburcio R, et al. (2007) Characterization of necrosis and ethylene-inducing proteins (NEP) in the basidiomycete *Moniliophthora perniciosa*, the causal agent of witches' broom in *Theobroma cacao*. Mycol Res 111:443–455
12. Gesteira A, Micheli F, Carels N, et al. (2007) Comparative analysis of expressed genes from cacao meristems infected by *Moniliophthora perniciosa*. Ann Bot 100:129–140

13. Goldstein J, Newbury D, Joy D, et al. (2003) Scanning electron microscopy and x-ray microanalysis. Vol 3. Springer Science+Business Media, New York
14. Griffith GW, Nicholson J, Nenninger A, et al. (2003) Witches' brooms and frosty pods: two major pathogens of cacao. New Zeal J Bot 41:423–435
15. Guimaraes RL, Stotz HU (2004) Oxalate production by *Sclerotinia sclerotiorum* deregulates guard cells during infection. Plant Physiol 136:3703–3711
16. Han Y, Joosten HJ, Niu WL, et al. (2007) Oxaloacetate hydrolase, the C-C bond lyase of oxalate secreting fungi. J Biol Chem 282:9581–9590
17. Kesarwani M, Azam M, Natarajan K, et al. (2000) Oxalate decarboxylase from *Collybia velutipes*—molecular cloning and its overexpression to confer resistance to fungal infection in transgenic tobacco and tomato. J Biol Chem 275:7230–7238
18. Kubicek CP, Schreferlkunar G, Wohrer W, et al. (1988) Evidence for a cytoplasmic pathway of oxalate biosynthesis in *Aspergillus niger*. Appl Environ Microbiol 54:633–637
19. Lenz H, Wunderwald P, Eggerer H (1976) Partial purification and some properties of oxalacetase from *Aspergillus niger*. Eur J Biochem 65:225–236
20. Maximova SN, Marelli JP, Young A, et al. (2006) Over-expression of a cacao class I chitinase gene in *Theobroma cacao* L. enhances resistance against the pathogen, *Colletotrichum gloeosporioides*. Planta 224:740–749
21. Meinhardt LW, Bellato CD, Tsai SM (2001) SYBR (R) Green I used to evaluate the nuclei number of fungal mycelia. Biotechniques 31:42–46
22. Munir E, Yoon JJ, Tokimatsu T, et al. (2001) A physiological role for oxalic acid biosynthesis in the wood-rotting basidiomycete *Fomitopsis palustris*. Proc Natl Acad Sci USA 98:11126–11130
23. Pedersen H, Christensen B, Hjort C, et al. (2000) Construction and characterization of an oxalic acid nonproducing strain of *Aspergillus niger*. Metab Eng 2:34–41
24. Pennman D, Britton G, Hardwick K, et al. (2000) Chitin as a measure of biomass of *Crinipellis perniciosa*, causal agent of witches broom disease of cocoa. Mycol Res 104:671–675
25. Purdy LH, Schmidt RA (1996) Status of cacao witches' broom: biology, epidemiology, and management. Annu Rev Phytopathol 34:573–594
26. Rincones J, Meinhardt LW, Vidal BC, et al. (2003) Electrophoretic karyotype analysis of *Crinipellis perniciosa*, the causal agent of witches' broom disease of *Theobroma cacao*. Mycol Res 107:452–458
27. Scarpari LM, Meinhardt LW, Mazzafera P, et al. (2005) Biochemical changes during the development of witches' broom: the most important disease of cocoa in Brazil caused by *Crinipellis perniciosa*. J Exp Bot 56:865–877
28. Sexton AC, Cozijnsen AJ, Keniry A, et al. (2006) Comparison of transcription of multiple genes at three developmental stages of the plant pathogen *Sclerotinia sclerotiorum*. FEMS Microbiol Lett 258:150–160
29. Silva SDVM, Matsuoka K (1999) Histologia da interação *Crinipellis perniciosa* em cacaueiros suscetível e resistente à vassoura-de-bruxa. Fitopat Bras 24:54–59
30. Tokimatsu T, Nagai Y, Hattori T, et al. (1998) Purification and characteristics of a novel cytochrome c dependent glyoxylate dehydrogenase from a wood-destroying fungus *Tyromyces palustris*. FEBS Lett 437:117–121
31. Whitney KD, Arnott HJ (1986) Calcium oxalate crystals and basidiocarp dehiscence in *Geastrum saccatum* (Gasteromycetes). Mycologia 78:649–656
32. Whitney KD, Arnott HJ (1987) Calcium oxalate crystal morphology and development in *Agaricus bisporus*. Mycologia 79:180–187